SUPPORTING INFORMATION

2D CHIRAL STRUCTURES IN QUINOLEINE MIXED LANGMUIR MONOLAYERS.

Carlos Rubia-Payá[a], Juan J. Giner-Casares[a,b], María T. Martín-Romero[a], Dietmar Möbius[c] and Luis Camacho[a]

[a]*Institute of fine chemistry and nanochemistry. Department of Physical Chemistry and Applied Thermodynamics, University of Córdoba, Campus Universitario de Rabanales, Edificio Marie Curie, Córdoba, Spain E-14014*

[b]*Present address: Bionanoplasmonics Laboratory, CIC biomaGUNE, Paseo de Miramón 182, 20009 Donostia - San Sebastián, Spain.*

[c]*Max-Planck-Institut für biophysikalische Chemie, Am Fassberg 11, D-37077 Göttingen, Germany*

Index

1. Experimental and theoretical detailed procedures.

1.1.Extended dipole model.

The extended dipole model requires the assumption of considering molecules as their transition dipoles, $\mu = l \times q$, with fixed dipole length (l) and charge (q).[1-5]

Formation of infinite lineal aggregates of the HQ polar headgroups is assumed. Within these aggregates, the relative arrangement of two neighbors HQ groups is calculated from the final result of the molecular mechanics simulation. Figures 7D and 7E in the paper show the distribution used, result of averaging the determined parameters after 5 different computations. The red and orange arrows represent the transition dipoles of two consecutive molecules.

Given a quinoleine reference molecule, 1, the average excitation energy of this molecule due to the aggregation with N neighbor MQ molecules can be expressed as;

$$\Delta E_N = \Delta E_{mon} + 2\sum_{i=2}^{N} J_{1i}\frac{2\left(N+1-i\right)}{N} \qquad \text{(SI-1)}$$

where ΔE_{mon} is the excitation energy of the MQ monomer, and J_{1i} is the interaction energy between the dipoles corresponding to the reference molecule and each i molecules of the lineal aggregate, which can be expressed in an approximately way by;

$$J_{1i} = \frac{q^2}{D}\left[\frac{1}{a_{1i}} + \frac{1}{b_{1i}} - \frac{1}{c_{1i}} - \frac{1}{d_{1i}}\right] \qquad \text{(SI-2)}$$

$D \approx 2.5$ the dielectric constant, and a_{1i}, b_{1i}, c_{1i} and d_{1i} are the distances between ends of the dipoles positive–positive, negative–negative, positive–negative and negative–positive, respectively. Thus, the maximum wavelength of the aggregate λ_N, is;

$$\lambda_N = \frac{\lambda_{mon} hc10^7}{hc10^7 + 4\sum_{i=2}^{N} J_{1i} \frac{(N+1-i)}{N}} \qquad \text{(SI-3)}$$

For the λ_3 mode λ_{mon} = 242 nm the maximum wavelength of monomer, i.e., in absence of aggregation. The application of this model requires the previous knowledge of l, q, and μ. The value $\mu = l \times q$ = 5.17 Debye for the transition dipole that has been obtained by integrating the absorption band in solution (oscillator strength, f = 0.329). When $N \rightarrow \infty$ and l = 0.3 nm and q = 0.36 e, λ_N = 238 nm is obtained, in good agreement with the experimental data, see Figure 5 in the paper. Similar calculations using the λ_1 and λ_2 modes lead to maximum wavelength displacement lower than 2 nm.

1.2. Experimental parameters for tuning the shape and size of the chiral domains.

We have observed that using freshly prepared solutions, and allowing a waiting time before compressing the monolayer of 45 minutes, assures a good reproducibility of the results. No homogeneous domains distribution was obtained in any experiment. Additional experimental parameters have been analyzed: spreading solvent, concentration of spreading solution, and temperature of the liquid subphase. The variation in these experimental parameters does not lead to significant changes in the experimental results, as shown in Figures 3 and 4 of the paper. Note that during the

phase transition the monolayer moves quickly under the BAM focus, thus the evolution of the domains is difficult to be followed in great detail.

Experimental parameters for the results showed in Figure 8 and 9 of the paper are defined as follows;

Compression rate (nm^2 min^{-1} $molecule^{-1}$)	
Slow	0.04
Fast	0.80

Point	Figure 8 and Figures 9A-9C	Figure 9-d	Figure 9-e	Figure 9-f
B(π, mN/m)	6	6	6	6
D(π, mN/m)	9.5	11	12	9.5
E(π, mN/m)	6	6.5	7	7

2. Cyclic isotherms

Figure S1 (red line) shows the π-*A* isotherms of MQ:DMPA system during the first compression cycle. When the monolayer is decompressed (gray line), and a second compression process is realized (black dotted line) no hysteresis was observed.

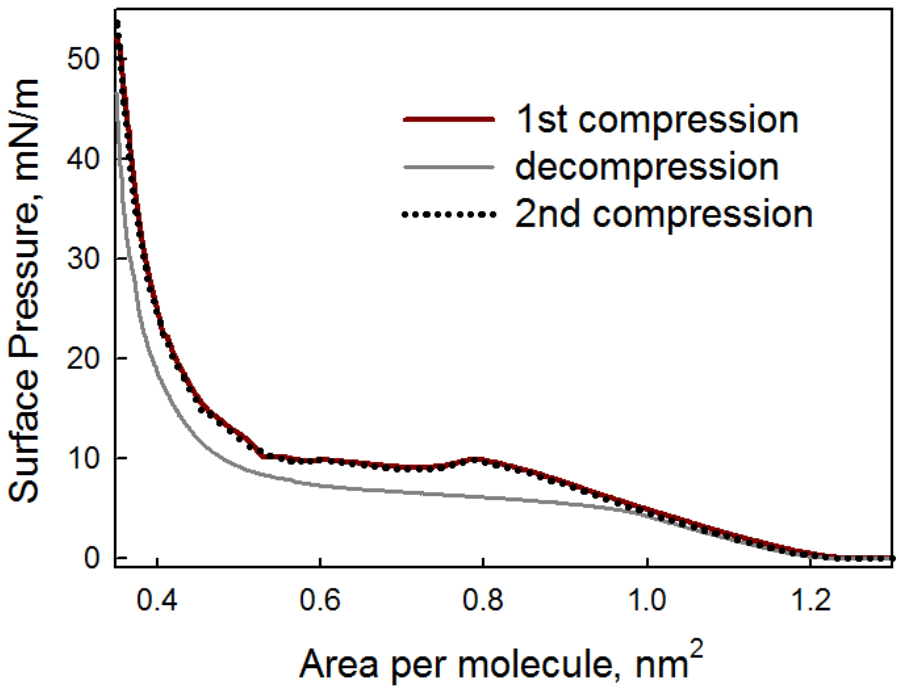

Figure S1. Surface pressure-area (π-A) isotherms of the mixed MQ:DMPA monolayer. Red line: first compression cycle. Gray line: decompression process. Black dotted line: Second compression cycle. T = 21°C.

3. Variation of molar ratio MQ:DMPA in mixed Langmuir monolayers.

Figure S2 shows the π-*A* isotherms of MQ:DMPA monolayers, obtained at various molar fractions of MQ. It has to be pointed out that the isotherm overshoot could not be observed for $x \neq 0.5$.

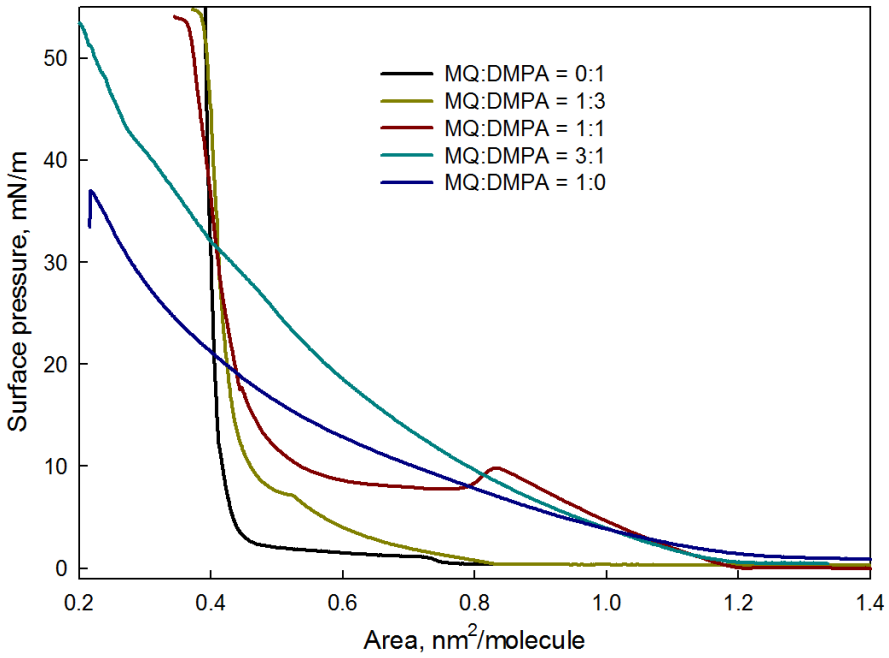

Figure S2. Surface pressure-area (π-A) isotherms of the mixed MQ:DMPA monolayer at various mole fractions of MQ(x) at T = 21°C.

4. UV-Visible spectrum Simulation and bands assignment.

In order to simulate the MQ UV-Visible spectrum and obtain the transition dipoles orientation, the geometry molecule was previously optimize by using the RM1 semi-empirical method.[6] Then, the UV-Visible spectrum was simulated in vacuum, using the ZINDO/S-CI semi-empirical method,[7] with $OWP_{\pi\text{-}\pi}$ = 0.58 (Overlap Weighting Factor). This semi-empirical method is designed to reproduce UV-Visible spectra of organic molecules, showing an accuracy similar to the Density Functional methods.[8] Both calculations were performed using the commercial software Hyperchem 8.0.[9]

By this procedure the transitions between the 8 OM occupied of highest energy and 8 OM unoccupied of lower energy were obtained. In this simulation a total of 128 possible transitions, 64 singlets ($\Delta S=0$) and 64 triplets ($\Delta S=1$) were analyzed. Of these transitions only 3 have wavelength λ_{max} > 240 nm, and oscillator strength different of zero (allowed transitions) which are shown in Figure S3. These transitions correspond to the modes λ_1, λ_2 and λ_3, observed in the experimental spectrum.

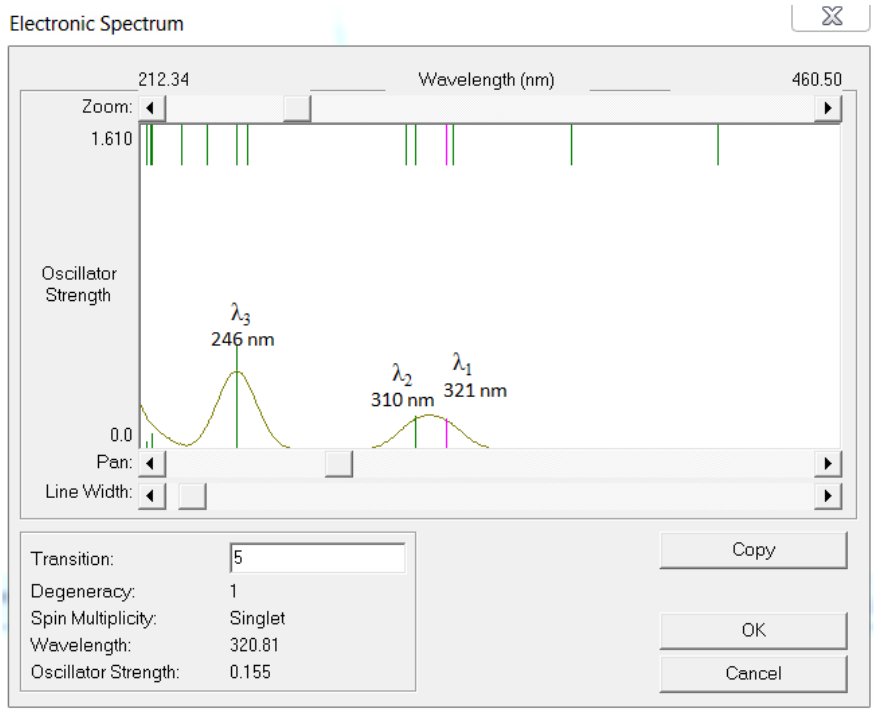

Figure S3: *In vacuo* simulated UV-Vis spectrum of MQ by using Hyperchem 8.0.

REFERENCES

(1) Czlikkely, V.; Forsterling, H. D.; Kuhn, H. *Chem. Phys. Lett.* **1970**, 6, 11.

(2) Czikklely, V.; Forsterling, H. D.; Kuhn, H. *Phys. Lett.* **1970**, 6, 207.

(3) Pedrosa, J. M.; Martín-Romero, M. T.; Camacho, L.; Möbius, D. *J. Phys. Chem. B* **2002**, 106, 2583.

(4) de Miguel, G.; Martín-Romero, M. T.; Pedrosa, J. M.; Muñoz, E.; Pérez-Morales, M.; Richardson, T. H.; Camacho, L. *Phys. Chem. Chem. Phys.* **2008**, 10, 1569.

(5) Giner-Casares, J. J.; de Miguel, G.; Perez-Morales, M.; Martin-Romero, M. T.; Camacho, L.; Munoz, E. *J. Phys. Chem. C* **2009**, 113, 5711.

(6) Rocha, G. B.; Freire, R. O.; Simas, A. M.; Stewart, J. J. P. *J. Comput. Chem.* **2006**, *27*, 1101.

(7) Neto, J. D. D.; Zerner, M. C. *Int. J. Quantum Chem.* **2001**, *81*, 187.

(8) Safarpour, M. A.; Navir, S. B.; Jamali, M.; Mehdipour, A. R. *J. Mol. Struct. (Theochem.)* **2009**, *900*, 19.

(9) Hyperchem; 8th ed.; Htpercube, Inc.: Gainesville, FL, 2007.